ELSEVIER

Ceramics International 25 (1999) 325–330

CERAMICS
INTERNATIONAL

Sintering of mullite–alumina composites from diphasic precursors

Minghua Zhou*, J.M.F. Ferreira, A.T. Fonseca, J.L. Baptista

Department of Ceramic and Glass Engineering, UIMC, University of Aveiro, 3800, Aveiro, Portugal

Received 23 January 1998; accepted 17 March 1998

Abstract

The densification characteristics of diphasic mullite–alumina composite precursors (with 10 vol% excess alumina over the stoichiometric mullite composition) were studied by both pressureless and pressure-assisted sintering. The precursors were prepared by either a coprecipitation method or a colloidal method using different starting materials. However, independent of the preparation method used, high temperatures up to 1600°C were required to densify the precursors either by pressureless or pressure-assisted sintering. This sintering behaviour was mainly due to the presence of the excess alumina after the formation of mullite at around 1200°C, eliminating the viscous phase and retarding the densification. For the coprecipitated precursor, the excess alumina precipitated out in the form of platelets in the pressureless sintering; the morphology of the alumina grains is less typical in the pressure-assisted sintered microstructure due to a change of the relation between densification and grain growth caused by the applied pressure. © 1999 Elsevier Science Limited and Techna S.r.l. All rights reserved.

Keywords: Mullite–alumina composite; Densification; Pressure-assisted sintering

1. Introduction

A great deal of research work has been devoted to mullite ceramics in the past few decades, including different starting materials and different techniques used to prepare monophasic and diphasic mullite precursors in order to lower the mullitization temperature [1]. Since the alumina components and silica components were mixed at a molecular scale in the monophasic precursors, the mechanism of mullitization is a nucleation process and can take place at a temperature as low as 980°C. However, the expensive sources of alumina and silica limited its practical importance. From an industrial point of view, diphasic mullite precursors are more attractive due to the less expensive alumina and silica sources. On the other hand, the higher metastable energy available in the diphasic precursors, compared to the monophasic precursors, leads to enhanced sintering for diphasic precursors as studied by Komarneni et al. [2]. Some investigations starting with monophasic or diphasic mullite precursors are related to phenomena, such as crystallization of mullite [3–5], phase transitions [6,7], sintering of crystallised mullite [8,9], and mechanical properties of mullite ceramics [9–11]. The mullite phase is usually formed at 1200°C from diphasic precursors and can be sintered to high density at ~1250°C by viscous flow sintering as described by Scherer's model [12–14].

In the present work, the diphasic precursors used to study the sintering behaviours have 10 vol% excess alumina over the stoichiometric mullite composition. By analysing the effects of the excess alumina on the densification behaviour and the final sintered microstructures obtained by both pressureless and pressure-assisted sintering, the mechanisms of the densification are qualitatively discussed.

2. Experimental

A mullite–alumina composite precursor containing about 10 vol% excess alumina over the stoichiometric mullite composition was prepared by spraying a solution containing $AlCl_3$ and silicic acid, derived from sodium metasilicate by an ion exchange method, into a dilute ammonia solution maintained at pH 8.2 ± 0.2. Details of the preparation procedure and of the phase transitions observed during heating up of the obtained precursor have been reported earlier [15,16]. For comparison, another composite precursor with the same composition was also prepared by a colloidal method using $Al(NO_3)_3 \cdot 9H_2O$ (UN 1438, E. Merck, 64271 Darmstadt, Germany) and colloidal silica powder (Laboratory reagent, BDH Limited, Poole, UK). The

---

* Corresponding author.

PII: S0272-8842(98)00042-X

colloidal silica was dispersed into an ammonia solution with pH 11 (far away from the isoelectric point located in the pH range of 1–3), which could make the colloidal silica well dispersed, under strong mechanical stirring. This basic suspension was then acidified using a diluted HNO_3 solution. This silica sol was mixed with aluminium nitrate solution according to a composition of 10 vol% excess alumina over the stoichiometric mullite composition. The mixture solution was then sprayed into a dilute ammonia solution (pH ~8.5), using the same procedure adopted in the coprecipitation method, followed by the washing and filtration, conventional drying and calcination at different temperatures. The dried and calcined powders were analysed with a computer-controlled X-ray difractometer (Rigaku XDMAX) by using CuK_α radiation in the 10 to 70° 2θ-range at a scanning speed of 2° 2θ/min.

The powders calcined at 1000°C were planetary ball milled and used for both pressureless and pressure-assisted sintering.

The green bodies formed by uniaxial pressing (40 MPa), followed by isostatic pressing (150 MPa), were sintered at different temperatures (in the range of 1400–1600°C) for different dwelling times. The heating rate up to the sintering temperature was 5°C/min. The pressure-assisted sintering was performed in an induction heated furnace using graphite dies with a pressure of 25 MPa at 1400 and 1600°C, respectively, and a heating rate of 10°C/min from room temperature up to the holding temperatures. The pressure was loaded at 1300°C.

The sintered bulk densities were measured by the Archimedes displacement method using mercury. The sintered microstructures were observed by scanning electron microscopy (SEM) (Model S4100-1, Hitachi, Ltd., Tokyo, Japan) in polished sections of samples that had been previously thermally etched.

3. Results and discussion

3.1. Pressureless sintering

3.1.1. Characterisation of the precursors and densification behaviour

The diphasic characteristics of the mullite and mullite–alumina precursors prepared by the coprecipitation method have been reported earlier [15–18]. Some results concerning the phase transitions of the coprecipitated precursor are summarised in Table 1, confirming its diphasic nature. The coprecipitated and dried powder was mainly amorphous and only traces of poorly crystallised bayerite and boehmite could be detected. These phases disappeared after calcination at 350°C, and were transformed into amorphous or cryptocrystalline transient γ-alumina. The crystalline degree of this transition alumina was improved with increasing temperature. Some traces of θ-alumina also appeared after calcination at 1070°C. Beyond 1200°C mullite was the dominant phase with a very small amount of θ-alumina remaining, which disappears before 1400°C. At this calcination temperature mullite was the only identifiable phase present, but at 1500°C traces of α-alumina appeared together with a well-crystallised mullite phase.

The relative density of the compacts pressureless sintered from the coprecipitated precursor versus sintering temperature (the soaking time is 6 h) and versus sintering time at 1600°C are shown in Figs. 1 and 2, respectively. Since the alumina-containing species and the silica-containing species in this diphasic precursor are mixed at a nanometer scale, when the green body is sintered at 1400°C, mullite is formed and the grain growth (mullitization temperature 1200°C) takes place at local regions being controlled by the near-interface diffusion or by the interfacial reaction. However, the existence of the excess alumina over the stoichiometric composition in the precursor, which was entrapped in the mullite grains or distributed along the grain boundaries,

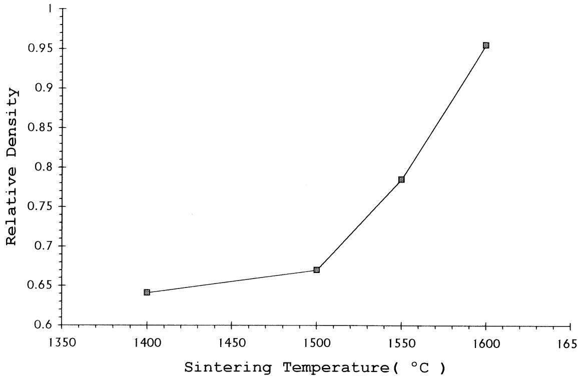

Fig. 1. Relative density versus sintering temperature for the coprecipitated precursor (6 h).

Table 1
Phase transitions of diphasic mullite–alumina composite precursor prepared by coprecipitation method

Temperature (°C)	120	350	850	1000	1070	1150	1200	1400	1500
Phases	Bayerite, Boehmite, AS	γ-Al_2O_3, AS	γ-Al_2O_3, AS	γ-Al_2O_3, AS	θ-Al_2O_3, AS	θ-Al_2O_4, AS	M, θ-Al_2O_3	M, θ-Al_2O_3	M, α-Al_2O_3
Average size of alumina crystallite (nm)	–	–	3.8	4.4	5.7	7.2	–	–	–

M, mullite; AS, amorphous silica.

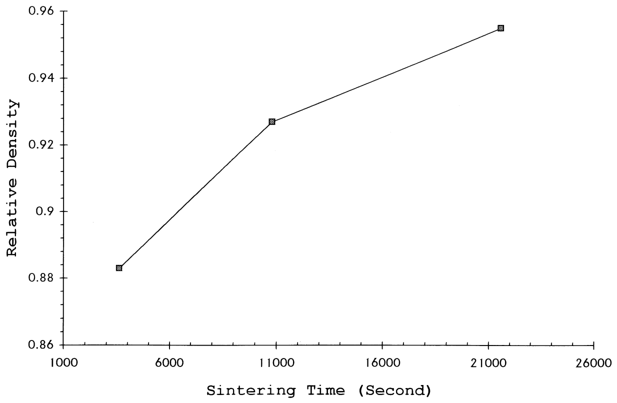

Fig. 2. Relative density versus sintering time for the coprecipitated precursor (1600°C).

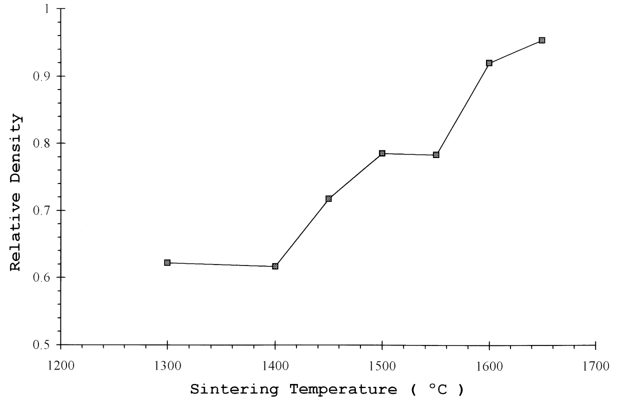

Fig. 3. Relative density versus sintering temperature for the colloidal precursor (6 h).

could reduce the quantity of the vitreous grain boundary phase which is very important for promoting the densification and grain growth. The sintered density could only reach 65% of the theoretical density, as shown in Fig. 1. The densification at this stage was probably due to (i) plastic flow of the small mullite grains by dislocation movement; (ii) viscous flow of a still remaining vitreous grain boundary phase. Viscous flow is the mechanism responsible for the high density diphasic mullite precursor [12]. A significant increase in sintered densities was only observed when the sintering temperature was raised to 1550~1600°C. A relative density of 96% was obtained after sintering at 1600°C for 6 h. This densification behaviour was quite different from the diphasic mullite precursors with stoichiometric composition.

From the sintered density versus sintering time shown in Fig. 2, together with the observation of the grain growth of both mullite and alumina [17], it seems that besides the two mechanisms involved in the low temperature sintering process, other densification mechanisms become active, specially at 1600°C, the most probably being (iii) deformation of the grains by lattice diffusion (Nabarro–Herring creep), (iv) deformation by grain boundary diffusion (Coble creep). A similar sintering behaviour can be observed in Fig. 3 with the precursor prepared by the colloidal method which shows ~62% relative density obtained in the first densification stage starting at ~1400°C, while further densification needs temperatures around 1600°C.

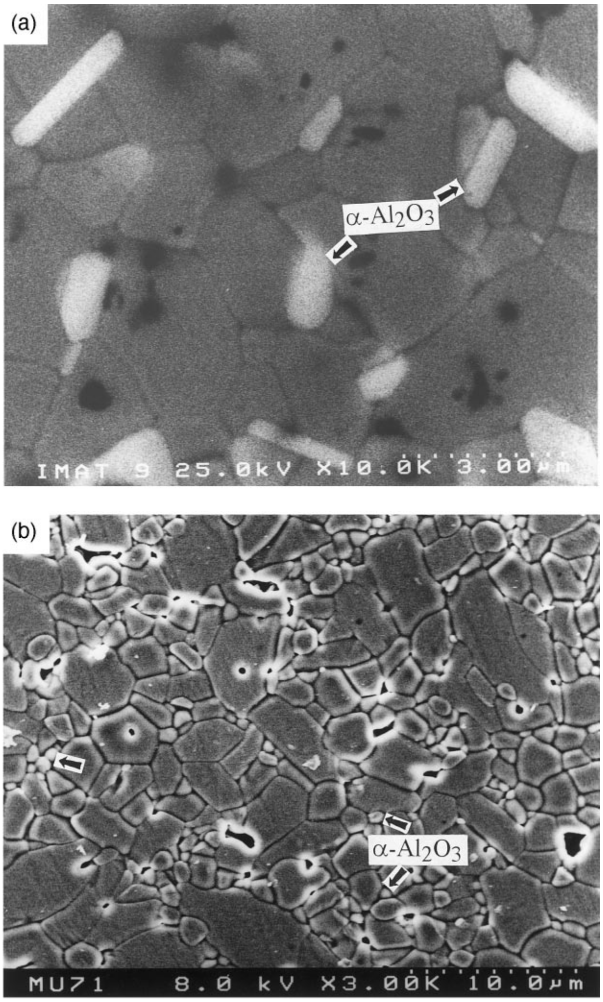

Fig. 4. SEM micrographs of the pressureless-sintered bodies at 1600°C for 6 h: (a) the coprecipitated mullite–alumina composite precursor (backscattering electron signal); (b) the colloidal mullite–alumina composite precursor (secondary electron signal).

3.1.2. Sintered microstructures

Fig. 4 shows the microstructures of the samples sintered at 1600°C from the precursors prepared by the coprecipitation method and by the colloidal method. As can be seen in Fig. 4(a), the excess alumina in the sample sintered from the coprecipitated precursor precipitated out in the form of α-Al_2O_3 platelets, while some pores are entrapped inside the mullite grains or distributed along the grain boundaries. A considerably different microstructure was obtained from the precursor prepared by the colloidal method as shown in Fig. 4(b). In this microstructure, the excess alumina is disseminated in the form of small equiaxial α-Al_2O_3

grains distributed at the triple points or along the grain boundaries, while some mullite grains appear with abnormal sizes. The abnormal mullite grain growth observed in the composite prepared from the colloidal precursor might derive from a less uniform distribution of the components in the mixture. More abundant liquid phase would occur where the concentration of silica species is higher, favouring the abnormal grain growth.

3.2. Pressure-assisted sintering

3.2.1. Densification behaviour

The sintering behaviour and final density depend on the starting packing density and the driving force available for densification. Pressure-assisted sintering experiments were carried out at 1400°C and at 1600°C for both precursors used in this work. It was observed that the relative density after pressure-assisted sintering for 1 h at 1400°C was only 67% (2 per cent units higher than that obtained in pressureless sintering for 10 h). Since the temperature of 1400°C is much lower than the temperature at which the eutectic in the mullite and silica system (≈1598°C) occurs, the densification would mainly involve particle re-arrangement and viscous flow at this temperature as in the case of the pressure assisted sintering of Si_3N_4 [18]. This pressure-assisted sintered sample was then resintered at 1600°C for 6 h, reaching a relative density of 90%. This densification level is even lower than that attained by the pressureless sintered sample at 1600°C for 6 h. This is probably due to the formation of a stable porous microstructure by the previous 1400°C sintering process that requires a higher temperature for the further densification.

When the precursors were pressure-assisted sintered at 1600°C, which is higher than the eutectic temperature of mullite–silica system, the densification behaviours became more complicated for both precursors because of the involvement of several densification mechanisms, and the quite different relation between the densification and grain growth, compared to the situation in the pressureless sintering. The densification curves are shown in Figs. 5 and 6. After holding at 1600°C for 1 h, almost full density was obtained.

3.2.2. Sintered microstructures

The micrographs of the pressure-assisted sintered microstructures are shown in Figs. 7 and 8. Both structures were well densified, with no visible pores, confirming the results of the density measurements. The morphology of the mullite grains in the sintered compact in Fig. 7(a) is not very different from the microstructure obtained by pressureless sintering for the coprecipitated precursors, as shown in Fig. 4(a). However, a completely different situation is observed concerning the alumina grains. The second phase-α-alumina appeared in the form of well defined platelets in pressureless sintering, while it is not so well defined in the pressure-assisted sintered sample. One of the possible reasons might be a different relation between the densification and the grain growth in the case of the pressure-assisted sintering.

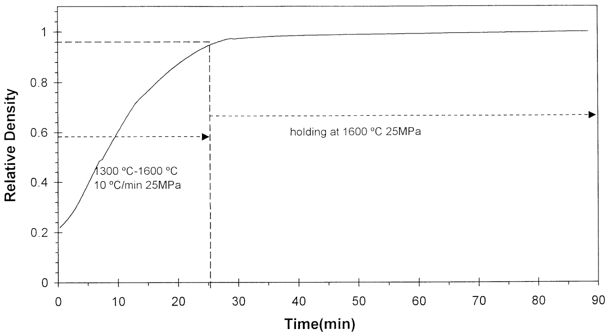

Fig. 5. Densification curve of the coprecipitated mullite–alumina composite precursor.

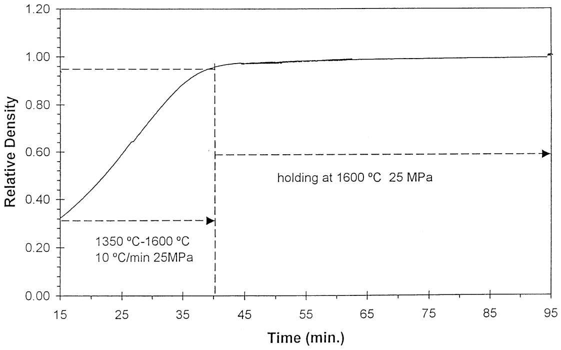

Fig. 6. Densification curve of the colloidal mullite–alumina composite precursor.

In pressureless sintering of diphasic stoichiometric mullite precursors obtained by coprecipitation, the mullite grains tend to grow along their preferred orientation and appear in an elongated form [19]. However, the presence of the excess alumina over the stoichiometric mullite composition used in the present work changed this tendency, as shown in Fig. 4(a). A uniform microstructure with equiaxial mullite grains and α-Al_2O_3 platelets was obtained. When the sintering was pressure-assisted, not well-defined fine mullite grains were densely compacted, the sporadic arrangement of the non-well-defined mullite grains due to external pressure changed the nucleation and grain growth behaviours in the case of pressureless sintering as reported earlier [17,19]. A high density was obtained at the holding temperature in a short time as shown in Fig. 5. The densification was promoted by the shortening of the diffusion paths while the grain growth was suppressed, giving a well-densified microstructure with small grain size. This would be the main reason why the platelet characteristic of the alumina grains is not as

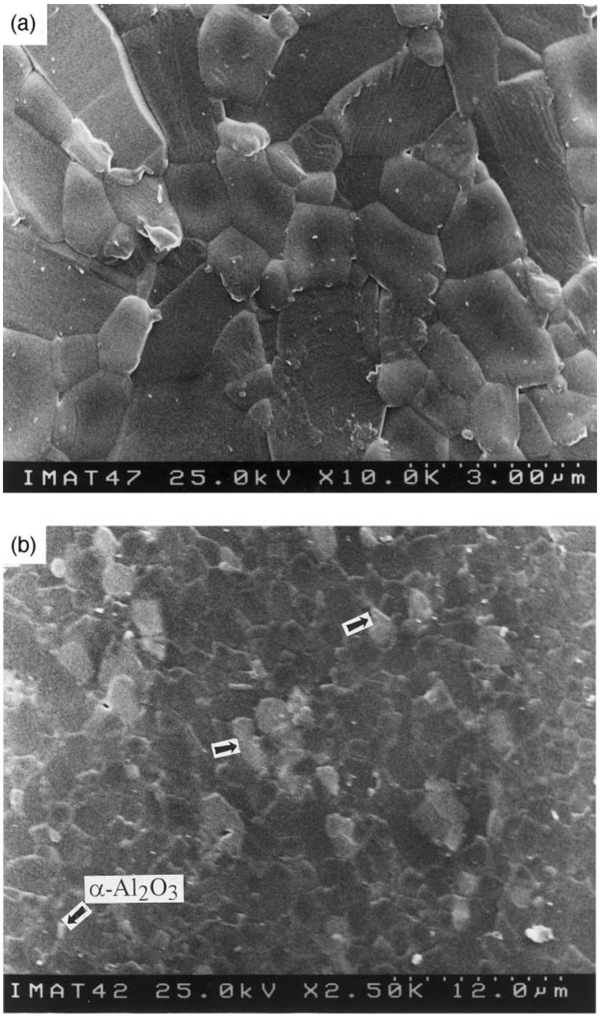

Fig. 7. SEM micrographs of the pressure-assisted sintered bodies from: (a) the coprecipitated mullite–alumina composite precursor; (b) the colloidal mullite–alumina composite precursor.

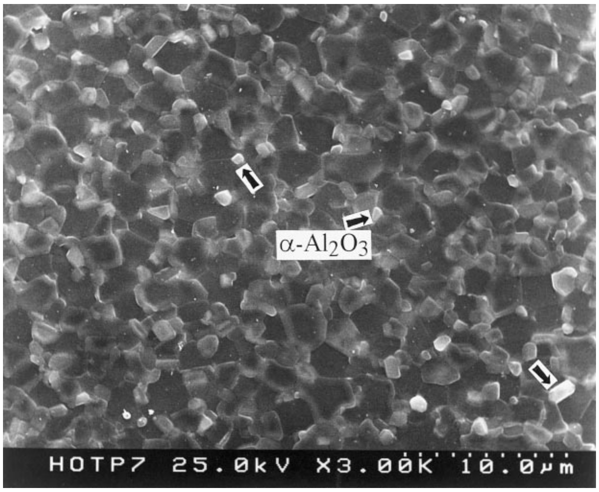

Fig. 8. SEM micrograph of the pressure-assisted sintered body from the colloidal mullite–alumina composite precursor.

typical as in the pressureless sintered microstructure, while the mullite grains kept its equiaxial morphology.

For the precursor prepared by the colloidal method, the pressureless sintered microstructure obtained at 1600°C for 6 h show small alumina grains embedded in a mullite matrix with some abnormal grain growth. As stated above, the modification of the relation between densification and grain growth in the pressure-assisted sintering where the long range diffusion process plays a less important role, enabled the obtention of a relatively uniform and fine microstructure after 1 h at 1600°C as shown in Fig. 7(b).

4. Summary

The densification of the diphasic mullite–alumina composite precursors requires high temperatures up to 1600°C either by pressureless sintering or pressure-assisted sintering. The requirement of this high temperature is mainly due to the presence of the excess alumina remaining after the mullitization (around 1200°C) that probably eliminates the vitreous phase and retards the densification. For the coprecipitated precursor, the excess alumina precipitated out in a form of platelets in the pressureless sintering; the morphology of the alumina grains is less typical in the pressure-assisted sintered microstructure which might be due to a change of the relation between densification and grain growth caused by the applied pressure.

Acknowledgement

The authors would like to thank Fundação para a Ciência e a Tecnologia of Portugal for financial support.

References

[1] H. Schneider, K. Okada, J.A. Pask, Mullite and Mullite Ceramics, John Wiley & Sons Ltd, Chichester, UK, 1994.
[2] S. Komarneni, Y. Suwa, R. Roy, Application of Compositionally diphasic xerogels for enhanced densification: the system Al$_2$O$_3$–SiO$_2$, J. Am. Ceram. Soc. 69 (7) (1986) C-155–C-156.
[3] W.-C. Wei, J.W. Halloran, Phase transformation of diphasic aluminosilicate gels, J. Am. Ceram. Soc. 71 (3) (1988) 166–172.
[4] W.-C. Wei, J.W. Halloran, Transformation kinetics of diphasic aluminosilicate gels, J. Am. Ceram. Soc. 71 (7) (1988) 581–587.
[5] S. Sundaresan, I.A. Aksay, Mullitization of diphasic aluminosilicate gels, J. Am. Ceram. Soc. 74 (10) (1991) 2388–2392.
[6] D.X. Li, W.J. Thomson, Tetragonal to orthorhombic transformation during mullite formation, J. Mater. Res. 6 (1991) 819–821.
[7] J.C. Hulling, G.L. Messing, Chemistry–crystallization relations in molecular mullite gels, J. Non-Cryst. Solids 213 (1992) 147–148.
[8] Y. Hirata, K. Sakeda, Y. Matsushita, K. Shimada, Y. Ishihara, Characterization and sintering behaviour of alkoxide derived aluminosilicate powders, J. Am. Ceram. Soc. 72 (6) (1989) 995–1002.
[9] T.J. Mroz Jr, J.W. Laughner, Microstructures of mullite sintered from seeded sol–gels, J. Am. Ceram. Soc. 72 (3) (1989) 508–509.

[10] I.A. Aksay, D.M. Dabbs, M. Sarikaya, Mullite for structural, electronic, and optical applications, J. Am. Ceram. Soc. 74 (10) (1991) 2343–2358.

[11] P.C. Dokko, J.A. Pask, K.S. Mazdiyasni, High temperature mechanical properties of mullite under compression, J. Am. Ceram. Soc. 60 (3–4) (1977) 150–155.

[12] L. Pash, A. Iratni, V. Kovar, P. Mankos, S. Komarneni, Sintering of diphasic mullite gel, J. Europ. Ceram. Soc. 16 (1996) 561–566.

[13] G.W. Scherer, C.J. Brinker, E.P. Roth, Sol–gel-glass: III viscous sintering, J. Non-Cryst. Solids 72 (1985) 369–389.

[14] G.W. Scherer, C.J. Brinker, E.P. Roth, Sintering of low density glasses (I, II, III), J. Am. Ceram. Soc. 60 (1977) 236–246.

[15] P.A. Caldeira, R.N. Correia, J.L. Baptista, In: P. Vincenzini (Ed.), Ceramics Today—Tomorrow's Ceramic Materials Science Monographs, Vol. 66B, Part B, Elsevier, Amsterdam, 1991, pp. 871–880.

[16] M. Zhou, J.M.F. Ferreira, A.T. Fonseca, J.L. Baptista, Wet chemical synthesis of nanocomposite powders in mullite–alumina system, Silicates Industriels 11–12 (1996) 249–252.

[17] M. Zhou, J.M.F. Ferreira, A.T. Fonseca, J.L. Baptista, "In-situ" formed α-alumina platelets in a mullite–alumina composite, J. Europ. Ceram. Soc. 18 (5) (1998) 495–500.

[18] L.J. Bowen, R.J. Weston, T.G. Carruthers, R.J. Brook, Hot-pressing and the α–β phase transforrmation in silicon nitride, J. Mater. Sci. 13 (1978) 341–350.

[19] M. Zhou, J.M.F. Ferreira, A.T. Fonseca, J.L. Baptista, Influence of the silica matrix on the formation of α-Al_2O_3 in mullite–alumina composite from diphasic precursor, J. Mater. Sci. 33 (7) (1998) 1851–1856.